Dissociation-Induced Depletion of High-Energy Reactant Molecules as a Mechanism for Pressure-Dependent Rate Constants for Bimolecular Reactions

Faraday Discussions (2022) https://doi.org/10.1039/D2FD00054G

Michael P. Burke,[1,2,*] Qinghui Meng,[1] Christopher Sabaitis[1]

[1]*Department of Mechanical Engineering, Columbia University*
[1]*Department of Chemical Engineering & Data Science Institute, Columbia University*
[*]*corresponding author: mpburke@columbia.edu*

In 1922, Lindemann proposed the now-well-known mechanism for pressure-dependent rate constants for unimolecular reactions: reactant molecules with sufficiently high energies dissociate more quickly than collisions can reestablish the Boltzmann distribution of the internal energies of the molecule during its dissociation at low pressures – yielding pressure-dependent rate constants for unimolecular reactions due to the preferential depletion of the high energy states capable of dissociation. In the last century, incredible progress has been made in achieving a far greater understanding of and quantitative predictions for unimolecular and association reactions. In the modern era, pressure-dependent phenomenological rate constants are now nearly universally used to describe the rates of unimolecular and associative reactions in phenomenological kinetic modeling. However, there is a second, more indirect, implication of Lindemann's mechanism that relates to how these dissociation-induced non-equilibrium distributions impact bimolecular reactions, including non-associative bimolecular reactions – which are generally not considered to have pressure-dependent rate constants. Yet, as we show herein, the same high energy states depleted due to dissociation would otherwise react most rapidly in high-activation-energy bimolecular reactions – yielding a mechanism for pressure-dependent rate constants for bimolecular reactions (including non-associative reactions). Here, we present results from a case study for CH_2O dissociation, isomerization, and bimolecular reaction with O_2 to explore this question. Results from our master equation calculations indicate that the effect of dissociation-induced non-equilibrium distributions on bimolecular reactions can be substantial – even when chemical timescales are well separated from internal energy relaxational timescales (i.e. when the traditional rate constant description would be thought to apply). This effect is found to be more pronounced – and more complex – for bimolecular reactions involving molecular entities whose chemical timescales are merged with the internal energy relaxational timescales. Finally, we present some ideas for discussion regarding what should be considered as "chemical species" in phenomenological kinetic models.

Introduction

Exactly 100 years ago at this very meeting, Lindemann made his seminal explanation for the observed pressure dependence of "unimolecular" reactions (i.e. those involving only one reactant engaging in bond transformations).[1] Using dissociation reactions as an example, he suggested that high-energy reactant molecules with sufficiently short lifetimes (relative to collision times) dissociate more quickly than it takes for collisions to reestablish the Boltzmann distribution of the internal energies of the molecule. Therefore, at low pressures with low collision frequencies, dissociation would preferentially deplete the population of the very energy states capable of reacting. By contrast, at high pressures, collisions may be sufficiently rapid relative to the microcanonical dissociation rate that the Boltzmann distribution is established for the reactant. The implication of this effect would of course be that the reaction rate could be independent of pressure at sufficiently high pressures but be dependent on pressure at sufficiently low pressures.

Specifically, the preferential depletion of reactive states due to dissociation would yield a lower rate constant for dissociation at lower pressures.

In the century that followed, an uncountably many studies (e.g. [2-17] and references therein) have established an impressive understanding – both qualitative and quantitative – of the manifestation of this competition among reactive and energy-transferring processes on the chemical evolution. In this regard, the master equation, which describes the temporal evolution of reactants on a microcanonical level, has elucidated the connection between these microscopic reactive and energy-transferring processes and the emergent (phenomenological) evolution of chemical species, including for reaction systems involving *n* potential energy wells. That is, under conditions where phenomenological rate constants exist, there are *n* slowly varying modes that describe the phenomenological chemical evolution of the *n* chemical species. The validity of this interpretation – and the phenomenological rate constant description itself – hinges on the commonly encountered separation of timescales for these chemical eigenmodes and those corresponding to internal energy relaxation.[5-8,11,14]

In such instances, the magnitudes of the eigenvalues (i.e. rates) of the internal energy relaxational eigenmodes (IEREs) are much larger than those for the chemically significant eigenmodes (CSEs). Then, provided that the reactants are not formed with very high energies, the vast majority of chemical reaction occurs after this internal energy relaxation period has ended. And so, the chemical evolution can be described by phenomenological rate constants for reactions among the *n* chemical species. Here, it is worth emphasizing that the non-equilibrium distributions describing the chemically significant eigenmodes and their eigenvalues – which influence phenomenological reaction rate constants – depend on the rates of reactive and energy-transferring processes, which in turn depend on the temperature (*T*) and, via the dependence of the energy-transfer rate, the pressure (*P*) and the composition of surrounding gas ($\underline{X}$).[10,17-19] Nowadays, *T/P/*$\underline{X}$-dependent phenomenological rate constants are nearly universally used to describe the rates of unimolecular and associative reactions in phenomenological kinetic modeling that describes the evolution of chemical species.

In the past few decades, a growing number of studies have then been devoted to situations where significant chemical reaction occurs on relaxational timescales. As alluded in the above paragraph, when reactants are formed from one potential energy surface with very high energies, they can react in subsequent potential energy surfaces on timescales comparable to energy relaxation (which is what is generally meant by the modern usage of the phrases “non-equilibrium,” “non-thermal,” or “non-Boltzmann”). For example, one or more of the bimolecular products formed from exothermic abstraction reactions can be formed with sufficiently high energy that they undergo prompt dissociation, isomerization, and/or bimolecular reaction prior to internal energy relaxation.[20-24] Weakly bound radicals, which often have Boltzmann distributions with significant populations of energy states above the dissociation threshold, are recognized to be especially prone to such effects.[21,24,25] Furthermore, the complexes formed from association of two species can be formed with sufficiently high energy that they undergo rapid bimolecular reaction with a third species prior to their dissociation or stabilization,[26-35] yielding chemically termolecular reactions involving three reactants engaged in the bond transformations.[31] In both of such instances, significant reactions across multiple potential energy surfaces occur on timescales that are comparable to internal energy relaxation, the manifestations of which continue to be the subject of considerable attention.

Additionally, under high temperatures and/or low pressures, one or more chemical reactions can be sufficiently rapid that the number of slowly evolving CSEs is less than the number of isomers, thereby "reducing" the number of distinct chemical species.[14,16,37] These chemical reactions, which describe the conversion of a reactant to another isomer and/or bimolecular products, are then said to "merge" with the quasi-continuum of IEREs (which are not resolved in phenomenological kinetics). How best to cope with this reduction in the number of chemical species is still recognized to be an important open question,[38] especially given that certain chemical species only exist over limited thermodynamic conditions and have distinct reactivity from its isomers.[37-40] For example, QOOH ceases to exist as a distinct chemical species under the conditions of interest to low-temperature combustion where its reactivity with O_2 plays an indispensable role.[30,38,39] Current treatments of such cases that include those molecular entities among the species in a phenomenological kinetic model are often premised on one of the isomers being maintained in partial equilibrium with another species and/or having rate constants that are extrapolated from conditions where they exist to conditions where they do not.

In this paper, we return to a second, more indirect, implication of the dissociation-induced non-equilibrium inherent to the Lindemann mechanism for unimolecular reactions – even in situations where insignificant reaction occurs on relaxational timescales and where the traditional phenomenological description is thought to apply. For context, at present, the dissociation-induced non-equilibrium of the reactants is generally only reflected in the *T/P/X*-dependent phenomenological rate constants for unimolecular and associative reactions in phenomenological kinetic modeling that describes the evolution of chemical species – which are otherwise considered to be *thermal*. However, this same dissociation-induced non-equilibrium of reactants is not generally considered for bimolecular reactions, including non-associative bimolecular reactions, which (aside from the formation of any inconsequential intermediate complexes that do not live long enough to undergo collisions) otherwise occur in a single step and are treated with a rate constant that depends only on temperature (*T*) – i.e. they are not considered pressure-dependent.

However, beyond the first (direct) implication on unimolecular and associative reactions, we note herein that this same dissociation-induced non-equilibrium also implies that the high energy states responsible for more rapid bimolecular reactions over a barrier are likely preferentially depleted by dissociation – including under circumstances where the conventional rate description is generally thought to apply. We therefore pose the question: what effect would this dissociation-induced non-equilibrium have on the phenomenological rate constants of bimolecular reactions?

Here, we present an initial exploration of this question for a reaction system involving unimolecular reactions on a CH_2O potential energy surface and bimolecular reactions of CH_2O and its isomers with O_2 (Fig. 1). For example, as illustrated in Fig. 2, dissociation of CH_2O leads to preferential depletion of the high energy states of CH_2O in the slowest CSE (the quasi-steady state distribution at the conditions of Fig. 2) below their fractions in the Boltzmann distribution. Those same (depleted) high energy CH_2O molecules would otherwise react more quickly with O_2 to yield products $P_{CH2O+O2}$ (with a ~40 kcal/mol barrier) than the lower energy CH_2O molecules. Consequently, the phenomenological rate constant for $CH_2O + O_2 \rightarrow P_{CH2O+O2}$ is lower than the thermal rate constant. Results from our master equation calculations indicate that the effect of dissociation-induced non-equilibrium on bimolecular reactions can be substantial – even in situations where the bimolecular reaction with O_2 is the dominant consumption pathway and where the values of the usual metrics for assessing the validity of the phenomenological rate constant description would not be thought to cause significant issues.

For example, we find deviations in the phenomenological rate constant for $CH_2O + O_2 \rightarrow P_{CH2O+O2}$ at 1 atm from the thermal rate constant of ~40% at conditions where the chemically significant eigenvalue is 100 times lower than the second largest eigenvalue and when the prompt dissociation fraction is less than 1%. Still, even with a prompt dissociation fraction of only 1%, this preferentially depleted tail of the energy distribution is responsible for reducing the rates of (high-activation-energy) bimolecular reactions in the same way it does for unimolecular reactions. These deviations are found to increase substantially with increasing temperature, where the prompt dissociation fractions become more significant (which is common for species at combustion temperatures) but the eigenvalues are still separated by an order of magnitude. Even still, when there remains a clear separation of the eigenvalues, high prompt reaction fractions are not thought to be immediately problematic[15] (provided that prompt reactions during the internal energy relaxational period following its formation are appropriately considered). However, we find deviations in the phenomenological rate constant for $CH_2O + O_2 \rightarrow P_{CH2O+O2}$ at 1 atm from the thermal rate constant at such conditions of a factor of three.

While the above paragraph focuses on the impact of preferential depletion on bimolecular reactions involving CH_2O, which would generally be thought to exist as a chemical species over the full set of conditions explored, we find still more profound (and multifaceted) impact for the bimolecular reactions involving *t*-HCOH and *c*-HCOH, whose timescales merge with the internal energy relaxational ones around ~2000 K and cease to exist as chemical species. While the reactions of *t*-HCOH and *c*-HCOH with O_2 do not depend as strongly on the reactant internal energy, our results indicate that rate constants calculated according to usual methods for treating the bimolecular reactivity of molecular entities that do not exist as chemical species – which assume that they are in chemical equilibrium with other isomers and engage in thermal bimolecular reactions – are in error by two orders of magnitude.

Below, we describe our master equation methodology for simulating the unimolecular reactions, bimolecular reactions, and energy-transferring processes of the CH_2O/*t*-HCOH/*c*-HCOH + M/O_2 reaction system. We then present results from these calculations for the (1) semi-microcanonical rate constants for $CH_2O + O_2 \rightarrow P_{CH2O+O2}$ as a function of the internal energy of CH_2O and temperature, (2) eigenvalues and eigenvectors directly from diagonalization of the master equation transition matrix to understand the nature of the slowest eigenmodes and their relationships to chemical evolution, (3) prompt reaction fractions of CH_2O, *t*-HCOH, and *c*-HCOH, and (4) phenomenological rate constants for the reactions among the various considered chemical species and the relationship between their phenomenological rate constants (collectively) with the thermal rate constants that would be calculated via canonical transition state theory.

Methodology

The time evolution of the populations of each isomer, *i* (with *i* = CH_2O, *t*-HCOH, and *c*-HCOH), on a discretized domain of rovibrational energy, *E,* as they undergo unimolecular dissociation reactions, unimolecular isomerization reactions, bimolecular reactions with O_2, and collisional energy transfer with the surrounding bath gas and/or are formed from bimolecular association reactions, is described by a single master equation using an overall methodology similar to our previous work.[34] Following a nomenclature similar to Georgievskii et al.,[16] the time evolution of the population of each isomer *i* at each energy *E*, $f_i(E,t)$, can be described by

$$\frac{\partial f_i(E,t)}{\partial t} = \int Z_i(T)P_i(E' \to E;T)f_i(E',t)dE' - Z_i(T)f_i(E,t) + \sum_{j\neq i} k_{j\to i}(E)f_j(E,t) - \sum_{j\neq i} k_{i\to j}(E)f_i(E,t) - \sum_{\xi,\zeta} k_{i+\mathrm{C}^{(\xi)}\to\zeta}(E;T)f_i(E,t)n_{\mathrm{C}^{(\xi)}} - \sum_{\nu} k_{i\to\nu}(E)f_i(E,t) + \sum_{\nu} k_{\nu\to i}(E)n_{\mathrm{A}^{(\nu)}}n_{\mathrm{B}^{(\nu)}}\rho_\nu(E)\exp(-E/k_BT)/Q_\nu(T) \quad (1)$$

where $Z_i(T)$ is the collision rate of isomer *i* with the bath gas at temperature *T*; $P_i(E' \to E;T)$ is the probability of a collision inducing a transition from *i* with energy *E'* to *i* with rovibrational energy *E*; $k_{j\to i}(E)$ is the rate constant for isomerization from *j* with energy *E* to *i* and vice versa for $k_{i\to j}(E)$, $k_{i+\mathrm{C}^{(\xi)}\to p}(E;T)$ is the rate constant for isomer *i* with energy *E* reacting with each reactive species $\mathrm{C}^{(\xi)}$ to form product *ζ* (where $\mathrm{C}^{(\xi)} = \mathrm{O_2}$ and $\zeta = \mathrm{P_{CH2O+O2}}$, $\mathrm{P_{}t\text{-HCOH+O2}}$, and $P_{c\text{-HCOH+O2}}$ here), $n_{C^{(\xi)}}$ is the concentration of each reactive species $\mathrm{C}^{(\xi)}$, $k_{i\to\nu}(E)$ is the rate constant for dissociation of *i* with energy *E* to each pair of bimolecular species ν (where ν = H + HCO, $\mathrm{H_2}$ + CO here), $k_{\nu\to i}(E)$ is the rate constant for association of $\mathrm{A}^{(\nu)}$ + $\mathrm{B}^{(\nu)}$ for each bimolecular pair ν to form isomer *i* with energy *E*, $n_{\mathrm{A}^{(\nu)}}$ and $n_{\mathrm{B}^{(\nu)}}$ are the concentrations of the ν bimolecular species $\mathrm{A}^{(\nu)}$ + $\mathrm{B}^{(\nu)}$, $\rho_\nu(E)$ is the density of states for $\mathrm{A}^{(\nu)}$ + $\mathrm{B}^{(\nu)}$, k_B is the Boltzmann constant, and $Q_\nu(T)$ is the partition function for $\mathrm{A}^{(\nu)}$ + $\mathrm{B}^{(\nu)}$. All bimolecular reactants, $\mathrm{A}^{(\nu)}$ and $\mathrm{B}^{(\nu)}$, and reactive collider species $\mathrm{C}^{(\xi)}$ are assumed to be thermally distributed and vary sufficiently slowly relative to internal-energy relaxation to be considered constant. The equation written above also treats the bimolecular reaction of *i* with $\mathrm{C}^{(\xi)}$ as irreversible, which is appropriate for the abstraction reactions considered here (and can be applied more generally – albeit approximately – through rate constants that consider only the forward direction[30,34,36]).

For all terms on the right-hand side of Eq. (1) except for the terms describing bimolecular reactions with $\mathrm{C}^{(\xi)}$, the present calculations make use of a previous characterization of unimolecular $\mathrm{CH_2O}$/*t*-HCOH/*c*-HCOH kinetics, whose potential energy surface is included as part of Fig. 1, and energy transfer from Klippenstein.[41] This treatment is based on high-level coupled-cluster-based transition state theory for the saddle points describing decomposition to $\mathrm{H_2}$ + CO and isomerization among $\mathrm{CH_2O}$, *t*-HCOH, and *c*-HCOH with tunneling corrections using the Eckart model. This treatment also employs multi-reference-based variable-reaction-coordinate transition state theory for the barrierless dissociation to H + HCO and associated long-range interactions that also result in roaming to $\mathrm{H_2}$ + CO. Finally, this characterization also uses the Lennard-Jones model for $Z_i(T)$ and a biexponential down model for $P_i(E' \to E;T)$, with parameters fitted to experimental data, to represent the collisional energy transfer function. Indeed, our master equation calculations using this characterization confirm that the resulting rate constants and branching ratios for $\mathrm{CH_2O}$ dissociation are in reasonable consistency with high-temperature experimental determinations from shock tube measurements near ~2500 K and ~1.6 atm.[42]

We then assemble a single master equation that includes both this treatment of the unimolecular kinetics and energy transfer and a treatment of the bimolecular reactions of *i* = $\mathrm{CH_2O}$, *t*-HCOH, and *c*-HCOH with $\mathrm{C}^{(\xi)}$ = $\mathrm{O_2}$ via reaction channels with pseudo-first-order rates given by $k_{i+\mathrm{C}^{(\xi)}\to\zeta}(E;T)n_{\mathrm{C}^{(\xi)}}$, where $k_{i+\mathrm{C}^{(\xi)}\to\zeta}(E;T)$ is a function of the rovibrational energy *E* of the isomer *i* and the temperature *T* (characteristic of the $\mathrm{C}^{(\xi)}$ co-reactant and the relative translation between *i* and $\mathrm{C}^{(\xi)}$).

For reaction of *i* = CH_2O with $C^{(\xi)}$ = O_2, which is known to proceed via a transition state with a barrier of ~40 kcal/mol and exhibits a strong temperature dependence,[42] the energy dependence of $k_{i+C^{(\xi)}\to\zeta}(E;T)$ would be expected to be significant (and would consequently result in pressure-dependent rate constants for $CH_2O + O_2 \rightarrow P_{CH2O+O2}$). Dynamics calculations, such as the classical trajectory calculations of Jasper et al.,[33] would provide the most accurate treatment of the effect of internal energy on the rate constant. On the other hand, statistical estimates, which make assumptions about how each mode contributes to the reaction coordinate, can be used to provide more affordable approximations. For example, Jasper et al.[33] compared the results for CH_4* + X (X = H, OH, O, O_2) from their trajectory calculations to statistical estimates based on their effective temperature model. They found that their effective temperature model reproduced their trajectory calculations within a factor of 2-3 for internal energies above 50 kcal/mol (where the rate constants are on the order of 10^{-11} cm^3 $molec^{-1}$ s^{-1} or more) and suggest that nonstatistical effects are small at such high energies and temperatures due to the rapid energy redistributions across various modes during reaction and large excess energy above the barrier.

The present calculations for CH_2O* + X employ the semi-microcanonical approach of Maranzana et al.[26] – an alternative statistical approach that makes similar assumptions but reproduces the thermal rate constants exactly for a thermal distribution of internal energy in *i,* i.e. for $f_{CH_2O}(E) = f^{(0)}_{CH_2O}(E;T)$. Our calculations shown in Fig. S1 of the Electronic Supporting Information show that this statistical approach agrees similarly well with the dynamics calculations of Jasper et al.[33] (within a factor of 2-3 above 50 kcal/mol). Consequently, the combination of exactly reproducing the thermal rate constants for thermally distributed reactants and reasonably approximating the energy dependence of $k_{i+C^{(\xi)}\to\zeta}(E;T)$ make it a suitable approach for the present purpose of calculating the deviation of rate constants from the thermal case due to dissociation-induced depletion of states with internal energies above ~80 kcal/mol (where the predicted rate constants are on the order of 10^{-11} cm^3 $molec^{-1}$ s^{-1} or more, cf. Fig. 3).

Within the semi-microcanonical approach, $k_{i+C^{(\xi)}\to\zeta}(E;T)$ is calculated according to

$$k_{i+C^{(\xi)}\to\zeta}(E;T) = \int k_{i+C^{(\xi)}\to\zeta}(E,E')f^{(0)}_{C^{(\xi)}+tr}(E';T)dE' \quad (2)$$

where $k_{i+C^{(\xi)}\to\zeta}(E,E')$ is the rate constant for $i + C^{(\xi)} \to \zeta$ for given rovibrational energy *E* of *i* and energy *E′* in the rovibrational modes of $C^{(\xi)}$ and relative translation between *i* and $C^{(\xi)}$ combined; $f^{(0)}_{C^{(\xi)}+tr}(E') = \rho_{C^{(\xi)}+tr}(E')\exp(-E'/k_BT)/Q_{C^{(\xi)}+tr}$ is the Boltzmann distribution for the rovibrational modes of $C^{(\xi)}$ and relative translation between *i* and $C^{(\xi)}$ combined and $\rho_{C^{(\xi)}+tr}(E')$ and $Q_{C^{(\xi)}+tr}$ are, respectively, the density of states and partition function for the same with

$$\rho_{C^{(\xi)}+tr}(E') = \int \rho_{C^{(\xi)}}(x)\rho_{tr}(E'-x)dx \quad (3)$$

being the convolution of the density of states of the internal modes of $C^{(\xi)}$, $\rho_{C^{(\xi)}}$, and the relative translation between *i* and $C^{(\xi)}$, ρ_{tr}. For $k_{i+C^{(\xi)}\to\zeta}(E,E')$, the semi-microcanonical approach[26] assumes that $k_{i+C^{(\xi)}\to\zeta}(E,E') \approx k_{i+C^{(\xi)}\to\zeta}(E'')$ is a function of only the total energy contained in the internal modes of *i*, the internal modes of $C^{(\xi)}$, and their relative translation, $E'' = E + E'$, with

$$k_{i+C^{(\xi)}\to\zeta}(E'') = \frac{1}{h}\frac{N^{\#}_{i+C^{(\xi)}\to\zeta}(E'')}{\rho_{i+C^{(\xi)}}(E'')} \quad (4)$$

where *h* is Planck's constant and $\rho_{i+C^{(\xi)}}$ is the density of states for $i + C^{(\xi)}$ (including the internal modes of *i* and $C^{(\xi)}$ and their relative translation). As mentioned above, $k_{i+C^{(\xi)}\to\zeta}(E;T)$ calculated using this approach exactly reproduces the thermal rate constant, $k_{i+C^{(\xi)}\to\zeta}(T)$, if the energy distribution of *i* is taken to be the Boltzmann distribution, $f_i^{(0)}(E;T)$, at the same temperature *T*. Indeed, the thermal rate constants (corresponding to the high-pressure, low-O_2 limit) calculated using our master equation model were confirmed to be the same as those predicted by canonical transition state theory for the thermal rate constants.

For the reaction of HCOH with O_2, which our limited electronic structure theory calculations suggest occurs with little to no barrier and therefore exhibits only modest temperature dependence, $k_{t\text{-HCOH(+O2)}}(E,T)$ and $k_{c\text{-HCOH(+O2)}}(E,T)$ are simply taken to be an energy- and temperature-independent value of 10^{-11} cm^3 molec^{-1} s^{-1}, which is representative of values from rough theoretical kinetics calculations.

Altogether, the master equation presented in Eq. (1) can then be expressed in vector form (following Georgievskii et al.[16])

$$\frac{\partial|f\rangle}{\partial t} = -\hat{G}|f\rangle + \sum_\nu n_{A^{(\nu)}} n_{B^{(\nu)}}/Q_\nu \left|p^{(\nu)}\right\rangle \tag{5}$$

where $\hat{G} = \hat{Z} + \hat{K}$ is the kinetic relaxation operator, consisting of the collisional relaxation operator $\hat{Z}$ and chemical reaction operator $\hat{K}$ describing isomerization, dissociation, and bimolecular reaction with $C^{(\xi)}$; and the last term describes the population gain from the association of the v^{th} bimolecular species pair with

$$p_i^{(\nu)}(E) = k_{\nu\to i}(E)\rho_\nu(E)\exp\left(-E/k_B T\right) \tag{6}$$

Under the following scalar product of any two state vectors $|g\rangle$ and $|f\rangle$ as

$$\langle g|f\rangle = \sum_i \int g_i(E) f_i(E)/f_i^{(0)}(E)\, dE \tag{7}$$

the kinetic relaxation operator $\hat{G}$ is self-adjoint

$$\left\langle f\middle|\hat{G}\middle|g\right\rangle = \left\langle g\middle|\hat{G}\middle|f\right\rangle \tag{8}$$

as a result of microscopic detailed balance, such that $\hat{G}$ has a complete set of orthogonal eigenvectors $|\lambda\rangle$ with associated eigenvalues Λ_λ.[16]

Calculations using a discretized version of this master equation (Eq. 1) for specified *T*, *P*, and n_{O2} (or $X_{O2} = n_{O2}/n_{tot}$) are then performed using the PAPR-MESS code[16] (where the reactions of *t*-HCOH and *c*-HCOH with O_2 are included via the "Escape" method with a constant pseudo-first-order rate and the reaction of CH_2O with O_2, which has a complex energy dependence, is included via a fictitious product channel with an effective number of states chosen to produce the energy-dependent pseudo-first-order rates). Results are shown below for temperatures from 1000 to 5000 K, a pressure of 1 atm (where there is strong preferential depletion of CH_2O, *t*-HCOH, and *c*-HCOH above the dissociation threshold), and for two different O_2 mole fractions, $X_{O2} = 10^{-7}$ and 0.209, to show behavior representative of the low-O_2 limit (where reaction with O_2 is not fast enough to perturb the eigenvectors and eigenvalues[34,43] from the $X_{O2} = 0$ case) and representative of the O_2 mole fraction in air, respectively.

Results and Discussion

The eigenvalues and eigenvectors, directly obtained by diagonalization of the master equation transition matrix, are presented in Figs. 4-7 to illustrate the key features of the system evolution and, more specifically, to understand the nature of the slowest eigenmodes and their relationships to chemical evolution to provide a context for interpreting the phenomenological descriptions (which are presented thereafter).

As indicated in Fig. 4, the three smallest eigenvalues (Λ_1, Λ_2, Λ_3) for the three-well system generally increase with increasing temperature, eventually reaching a plateau nearly converged with the lower end of the IERE range at higher temperatures, though the smallest eigenvalue (Λ_1) remains separated from the others by at least a factor of five at all temperatures.

At 1000 K, for $X_{O2} = 10^{-7}$ (as shown in Fig. 5 and in the solid lines in Fig. 4), the three smallest eigenvalues (Λ_1, Λ_2, Λ_3) for the three-well system remain separated from the fourth smallest eigenvalue (Λ_4) by a factor of at least ~15. As indicated in Fig. 6, the energy distributions of each isomer in each of these three eigenvectors (λ_1, λ_2, and λ_3) largely follow their respective Boltzmann distributions (if the latter are scaled to match the eigenvector amplitudes of that isomer in its ground state). From inspection of Figs. 5-6, the λ_3 eigenmode appears to describe isomerization reactions that serve to (at least partially) equilibrate *c*-HCOH with *t*-HCOH and CH_2O; the λ_2 eigenmode appears to describe relatively slower isomerization reactions that serve to (at least partially) equilibrate *c*-HCOH and *t*-HCOH with CH_2O; and the λ_1 eigenmode appears to describe the slowest dissociation of the (partially) equilibrated CH_2O/*t*-HCOH/*c*-HCOH to bimolecular products. Altogether, these results for 1000 K and $X_{O2} = 10^{-7}$ are largely representative of what would be considered a normal situation, where the three smallest eigenvectors describe the chemical evolution of three chemical species on timescales much slower than internal energy relaxation (IEREs) and would therefore be considered chemically significant eigenvectors (CSEs).

At higher temperatures, Λ_2 and Λ_3 approach within a factor of two of Λ_4 and each other around ~1500 to 2000 K. The energy distributions of each isomer in both λ_2 and λ_3 differ from their corresponding Boltzmann distributions and, in the case of CH_2O, show both noticeably positive and negative amplitudes for a single isomer – characteristic of IERE modes.[16] At these temperatures and higher, *c*-HCOH and *t*-HCOH cease to be distinct chemical species. There remains only one CSE (λ_1) that describes the chemical evolution of (partially) equilibrated CH_2O/*t*-HCOH/*c*-HCOH, which predominantly consists of CH_2O.

The eigenvalue for this slowest eigenmode, Λ_1, remains more than 1000 times lower than the other eigenvalues at temperatures below ~2000 K, 100 times lower below ~3000 K, 10 times lower below ~4500K, and 5 times lower below 5000 K. This eigenmode, which would generally be thought to correspond to CH_2O, would therefore be considered chemically significant and, likewise, CH_2O would be considered to be a well-defined chemical species across most, if not all, of the considered temperatures.

As indicated by the dotted lines in Fig. 4 (corresponding to $X_{O2} = 0.209$), the magnitudes of Λ_2 and Λ_3 are substantially higher for higher O_2 mole fractions, such as those present in air. In fact, Λ_2 and Λ_3 are comparable to Λ_4 across the whole temperature range for $X_{O2} = 0.209$, including 1000 K, where they are well separated for $X_{O2} = 10^{-7}$. Inspection of the eigenvectors for $X_{O2} = 0.209$ at 1000 K (not shown) reveals even non-thermal energy distributions in λ_3 and noticeably positive and negative amplitudes of CH_2O in λ_3 (characteristic of IEREs). On the other hand, Λ_1 is noticeably higher for $X_{O2} = 0.209$ than for $X_{O2} = 10^{-7}$ (indicating that reaction with O_2 leads to faster disappearance of the partially equilibrated CH_2O/*t*-

HCOH/*c*-HCOH) but still remains well separated from the other eigenvalues across most, if not all, temperatures. At discussed further below, the energy distribution of CH_2O, the primary constituent of λ_1, in λ_1 for $X_{O2} = 0.209$ is nearly indistinguishable from its energy distribution for $X_{O2} = 10^{-7}$.

Summarizing the above results, with Λ_2 and Λ_3 nearly merged with the IEREs for most temperatures and O_2 mole fractions, *c*-HCOH and *t*-HCOH are not distinct chemical species for most temperatures and O_2 mole fractions. By contrast, Λ_1 would be considered chemically significant and CH_2O would be generally considered to exist as a chemical species across most, if not all, temperatures and O_2 mole fractions. Therefore, for our present purposes, we will consider CH_2O to be a representative "well-defined" chemical species and *c*-HCOH and *t*-HCOH to be representative of molecular entities that are not distinct chemical species in this present case study. The results and discussion below therefore focus on λ_1 as the CSE of interest (and only existing CSE for most temperatures and O_2 mole fractions). Likewise, the results in Figs. 8-11 apply a phenomenological description based in this one CSE such that the phenomenological reactions consist of unimolecular decomposition of the chemical species "CH_2O"

$$CH_2O \leftrightarrow H_2 + CO \quad \text{(R1)}$$

$$CH_2O \leftrightarrow H + HCO \quad \text{(R2)}$$

bimolecular-to-bimolecular reaction involving unimolecular decomposition of ephemeral CH_2O complexes formed from $H_2 + CO$

$$H_2 + CO \leftrightarrow H + HCO \quad \text{(R3)}$$

bimolecular reactions involving CH_2O/*t*-HCOH/*c*-HCOH reacting with O_2

$$CH_2O + O_2 \leftrightarrow P_{CH2O+O2} \quad \text{(R4)}$$

$$CH_2O + O_2 \leftrightarrow P_{t\text{-}HCOH+O2} \quad \text{(R5)}$$

$$CH_2O + O_2 \leftrightarrow P_{c\text{-}HCOH+O2} \quad \text{(R6)}$$

chemically termolecular reactions involving bimolecular reactions of ephemeral CH_2O/*t*-HCOH/*c*-HCOH complexes formed from $H_2 + CO$

$$H_2 + CO + O_2 \leftrightarrow P_{CH2O+O2} \quad \text{(R7)}$$

$$H_2 + CO + O_2 \leftrightarrow P_{t\text{-}HCOH+O2} \quad \text{(R8)}$$

$$H_2 + CO + O_2 \leftrightarrow P_{c\text{-}HCOH+O2} \quad \text{(R9)}$$

chemically termolecular reactions involving bimolecular reactions of ephemeral CH_2O/*t*-HCOH/*c*-HCOH complexes formed from H + HCO

$$H + HCO + O_2 \leftrightarrow P_{CH2O+O2} \quad \text{(R10)}$$

$$H + HCO + O_2 \leftrightarrow P_{t\text{-}HCOH+O2} \quad \text{(R11)}$$

$$H + HCO + O_2 \leftrightarrow P_{c\text{-}HCOH+O2} \quad \text{(R12)}$$

(and the second-order rate constants for R4-R6 and third-order rate constants for R7-R12 are obtained by dividing the pseudo-first-order rate constants for R4-R6 and pseudo-second-order rate constants for R7-R12 from the master equation by n_{O2}).

While Fig. 6 indicates that the energy distributions of the main isomer, CH_2O, in λ_1 (at most temperatures) are nearly thermal, it is of course important to note that the distributions are not exactly thermal. After all, the origin of pressure dependence in rate constants for unimolecular dissociation reactions is the preferential depletion induced by the dissociation itself. As indicated by Fig. 7, which compares the energy distributions of λ_1 (solid lines) and scaled Boltzmann distributions (dotted lines) for each isomer on a logarithmic scale, the energy distribution of CH_2O in λ_1 closely follows the Boltzmann distribution at low energies but is preferentially depleted at energies above the dissociation barriers (and even at energies somewhat below the dissociation barriers, attributable to both tunneling and weak collision effects). At lower temperatures where the Boltzmann distributions are concentrated at lower energies, the bulk of the energy distribution of CH_2O in λ_1 is relatively similar to the Boltzmann distribution for CH_2O. Indeed, as indicated in Fig. 8, the fraction of CH_2O that would promptly dissociate (or react with O_2) if initially formed in a Boltzmann distribution is less than 1% below 3000 K. At higher temperatures where the Boltzmann distributions have high populations at energies near and above the dissociation barriers, the energy distribution of CH_2O in λ_1 substantially differs from the Boltzmann distribution for CH_2O. Indeed, the prompt reaction fractions increase with temperature – reaching 20-25% at 5000 K. Even still, such high prompt reaction fractions would not usually be considered in itself problematic[15] (provided that prompt reactions during the internal energy relaxational period following its formation are appropriately considered), given that Λ_1 is still at least somewhat separated from Λ_2 (in fact, with Λ_2/Λ_1 greater than 10 below ~4500 K).

For *t*-HCOH and *c*-HCOH, which would not be considered distinct chemical species at most conditions here, the situation is obviously more complicated. In fact, as discussed in the Introduction, it remains an open question[38] about how to treat molecular entities which do not exist as chemical species but have distinct bimolecular reactivity from their isomers that do exist as chemical species. Available methods for treating the reactivity of such molecular entities usually involve considering the molecular entity among the chemical species in the phenomenological model, thermally equilibrated, and using rate constants extrapolated from conditions where it does exist as a chemical species and/or taken to be chemically equilibrated with the remaining isomer(s)[39] (though we note that this is not necessary if one is interested in only regimes where the entities do not exist as chemical species[30,36,44]). Assuming that *t*-HCOH and *c*-HCOH are present in thermal distributions and in chemical equilibrium with CH_2O would implicitly yield effective thermal rate constants for R5 and R6, $k_{5,t,eff}(T)$ and $k_{6,t,eff}(T)$, that are the product of the equilibrium constants for

$$CH_2O \leftrightarrow t\text{-HCOH} \quad \text{(R13)}$$

$$CH_2O \leftrightarrow c\text{-HCOH} \quad \text{(R14)}$$

and the thermal rate constants for

$$t\text{-HCOH} + O_2 \leftrightarrow P_{t\text{-HCOH+O2}} \quad \text{(R15)}$$

$$c\text{-HCOH} + O_2 \leftrightarrow P_{c\text{-HCOH+O2}} \quad \text{(R16)}$$

such that $k_{5,t,eff}(T) = K_{eq,13}(T)k_{15,t}(T)$ and $k_{6,t,eff}(T) = K_{eq,14}(T)k_{16,t}(T)$.

However, the results shown in Fig. 7 – which compare the energy-resolved amplitudes of *t*-HCOH and *c*-HCOH in λ_1 with their corresponding Boltzmann distributions scaled according to their relative proportions to CH_2O at chemical equilibrium – indicate two main problems with such a treatment. First, since their Boltzmann distributions are concentrated at even higher energies relative to their ground states than CH_2O, *t*-HCOH and *c*-HCOH show even stronger dissociation-induced non-equilibrium energy distributions than CH_2O. Second, while the higher order eigenmodes serve to *partially* equilibrate *t*-HCOH and *c*-HCOH with CH_2O, they also contribute to dissociation – such that the λ_1 eigenmode does not simply consist of chemically equilibrated CH_2O, *t*-HCOH, and *c*-HCOH. As depicted in Fig. 7, the proportions of *t*-HCOH and *c*-HCOH relative to CH_2O in λ_1 are lower than their respective chemically equilibrated fractions, and to an increasing extent with increasing temperature. Both of these attributes of *t*-HCOH and *c*-HCOH are reflected in their fractions of prompt dissociation and reaction with O_2 in Fig. 8 (where the remaining fraction corresponds to prompt isomerization to CH_2O according to their relative proportions in λ_1). In fact, the fraction of *t*-HCOH and *c*-HCOH that promptly isomerizes to CH_2O (or, alternatively, is projected onto λ_1) also corresponds to the ratio of the proportions of *t*-HCOH and c-HCOH per CH_2O in λ_1 to their proportions per CH_2O at chemical equilibrium.

For all isomers, including the generally "well-defined" CH_2O, the dissociation-induced non-equilibrium may be expected to impact the phenomenological rate constants for bimolecular reaction (particularly for bimolecular reactions with an energy barrier where the preferentially-depleted higher-energy states would have faster rates of bimolecular reaction, cf. Fig. 2-3). To address this question, Fig. 9 compares the phenomenological rate constant, $k_4(T,P,X_{O2})$, for $CH_2O + O_2 = P_{CH2O+O2}$ (R4) at 1 atm and $X_{O2} = 10^{-7}$ and 0.209 to the corresponding thermal rate constant, $k_{4,t}(T)$; Fig. 9 also compares the phenomenological rate constants, $k_5(T,P,X_{O2})$ and $k_6(T,P,X_{O2})$, for $CH_2O + O_2 = P_{t\text{-}HCOH+O2}$ (R5) and $CH_2O + O_2 = P_{c\text{-}HCOH+O2}$ (R6) to their corresponding effective thermal rate constants, $k_{5,t,eff}(T)$ and $k_{6,t,eff}(T)$. As the results show, the impact of dissociation-induced non-equilibrium on the bimolecular reaction rate constants, which are generally not considered to depend on pressure, can be substantial – even for "well-defined" chemical species like CH_2O. Specifically, the phenomenological rate constants at 1 atm fall below the thermal rate constants increasingly with increasing temperature. The rate constant for R4 (proceeding directly from the "well-defined" species CH_2O) at 1 atm is 40% lower than the thermal rate constant at 3000 K, where the prompt reaction fraction is less than 1% and Λ_1 is 100 times lower than Λ_2. The phenomenological rate constant for R4 at 1 atm is nearly 3 times lower than the thermal rate constant at ~4500 K, where the CH_2O prompt reaction fraction is large but Λ_1 is still 10 times lower than Λ_2. This substantially higher reduction of the bimolecular reaction than the prompt reaction fraction is attributable to the fact that the preferentially depleted high energy states would otherwise react more rapidly in high-activation-energy bimolecular reactions like R4.

The phenomenological rate constants for R5 and R6 (proceeding via *t*-HCOH and *c*-HCOH, which are not distinct chemical species) are, in general, lower than the effective thermal rate constants (which assume both thermal and chemical equilibrium among the isomers) by an even larger amount – the reduction reaches two orders of magnitude for high temperatures and/or high O_2 mole fractions. Given that *t*-HCOH + O_2 and *c*-HCOH + O_2 are considered to have energy-independent rate constants in the present calculations, the reduction in the rate constants for R5 and R6 directly corresponds to the ratio of their proportions per CH_2O in λ_1 relative to their proportions per CH_2O at chemical equilibrium (or, alternatively, their prompt isomerization fractions to CH_2O). (If instead *t*-HCOH + O_2 and *c*-HCOH + O_2 had a higher activation energy, the reduction could be much larger.)

While the dissociation-induced falloff of these bimolecular reactions is substantial, one might wonder whether these bimolecular reactions might simply be insignificant relative to dissociation anyway, so as to be of negligible importance. After all, bimolecular reactions with higher barriers (and bimolecular reactions involving higher energy isomers) would tend to be more strongly affected by the dissociation-induced non-equilibrium but would also occur at smaller rates such that they would be relatively less important to overall reactant consumption. On the contrary, the results in Fig. 10 indicate that R4 is the dominant consumption pathway for 1 atm and X_{O2} = 0.209 across all temperatures, including those where the phenomenological rate constant for R4 substantially differs from the thermal rate constant. Consequently, even bimolecular reactions with higher relative activation energies, for which the dissociation-induced falloff would be more pronounced, may still be competitive with dissociation. Furthermore, while the effective thermal rate constants for R5 and R6 would imply they would comprise 1-2% of the overall CH_2O consumption, their phenomenological rate constants at 1 atm indicate that they instead comprise a negligible fraction of overall CH_2O consumption – such that pressure dependence of R5 and R6 influences even their qualitative role.

Finally, it is worth pointing out that, while dissociation induces preferential depletion of the high energy states during dissociation to bimolecular fragments, those high energy states will be populated by bimolecular association reactions when those bimolecular fragments are both present. Those higher energy states can react with O_2 – phenomenologically yielding chemically termolecular reactions. At chemical equilibrium, the reactions of the higher energy complexes with O_2 (corresponding to chemically termolecular reactions) serve to fill the void in the CSE responsible for the reduced rate constants for bimolecular reactions of CH_2O with O_2. To illustrate this, Fig. 11 compares the thermal rate constants for $CH_2O + O_2$ with the phenomenological rate constants for $CH_2O + O_2$; the rate constants of the chemically termolecular reactions, $H_2 + CO + O_2$ and $H + HCO + O_2$, times the rate constants for $CH_2O \rightarrow H_2 + CO$ or $H + HCO$ divided by the rate constants for $H_2 + CO$ or $H + HCO \rightarrow CH_2O$ (representing the chemically termolecular reaction contributions at equilibrium); and their sum. The results indicate that the chemically termolecular reaction contributions are much smaller than the bimolecular reaction contributions for the cases where the reduction of the phenomenological rate constant for the bimolecular reaction from the thermal rate constant is small. On the contrary, the chemically termolecular reaction contributions are comparable to or larger than the bimolecular contributions when the reduction of the phenomenological rate constant for the bimolecular reaction from the thermal rate constant is substantial. In fact, the combined contributions of the bimolecular reaction and the chemically termolecular reactions at chemical equilibrium, also indicated in Fig. 11, is equal to the thermal rate constants for the reaction of each isomer with O_2 within a factor corresponding to the prompt reaction fraction (and the so-called non-equilibrium factor,[24] f_{ne}). For context, the rate constants for dissociation (k_1 and k_2) and those for the reverse bimolecular association reactions (k_{-1} and k_{-2}) from MESS differ from the equilibrium constant relation by this same factor, which is a common occurrence for phenomenological interpretations that effectively consider the CSE in a non-conservative, one-well ME to be the chemical species,[15] as is implemented in MESS.[16]) Summarizing the above discussion, chemically termolecular reactions, similar to well-skipping bimolecular reactions, proceed through the non-equilibrated states that are missing from the CSE (and, within the formalism of Georgievskii et al.,[16] belong in essence to the relaxational subspace) and therefore make up for the difference between the bimolecular phenomenological rate constants at 1 atm and the thermal rate constants.

Returning now to the main question of the present study: are even non-associative bimolecular reactions, which are essentially universally considered pressure-independent, actually pressure-dependent due to the same origins of pressure dependence for unimolecular and association reactions? The present results clearly indicate the answer is yes.

In fact, this appears to be true even for bimolecular reactions involving molecular entities considered to be well-defined chemical species, for conditions where the chemical timescales are considered well separated from the relaxational timescales, and in situations where the bimolecular reactions are major pathways.

The next natural question is: what does that mean? First of all, additional case studies of other prototypical reaction systems would be highly worthwhile – in order to determine how general such effects are and the system characteristics and thermodynamic conditions that are especially prone to such effects. There is reason to believe that there may be a limited range of activation energies for the bimolecular reactions where the pressure dependence is significant and the bimolecular reaction is competitive with dissociation – at least when bimolecular reactants that are generally well-defined chemical species. For bimolecular reactions involving reactants that are not well-defined chemical species, which appear likely to have much stronger deviation from the Boltzmann distributions, the situation is less clear.

More generally, since the time of Lindemann's suggestion, the dissociation-induced preferential depletion of a dissociating reactant has been increasingly recognized and understood to have a profound impact on its dissociation rate constant. The present results provide a compelling example of the importance of recognizing more generally that the molecular ensemble describing a dissociating reactant (i.e. the CSE) under low-dissociative-product conditions is not the thermal species that it is often thought to be in phenomenological kinetic models, which are largely interpreted as describing the evolution of thermal species.

In this regard, we wonder whether a still more general recognition of the imperfect alignment of the CSEs – describing the slow, phenomenologically resolved chemical evolution – and the thermal species of a specific isomer (or equilibrated isomer groups) would be worthwhile. Specifically, it in some sense might be more appropriate to consider the CSEs to be the chemical species themselves and to be the quantities whose evolution is described in a phenomenological model. That would imply, for example, in multi-well systems that each of the CSEs may each have their own bimolecular reactions calculated from the ME. Likewise, reactions that form a particular isomer would need to be projected onto the CSEs. And determining a mole fraction of a particular isomer would require projecting the CSEs onto each isomer. While we put forward this notion for discussion, its implementation is obviously well beyond the scope of this paper. Interestingly, a more limited, but similar, version of this idea for one-well systems has found some utility for describing the long-timescale evolution of shock-heated, weakly bound radicals at high temperatures.[25] While it may at first glance seem unnecessarily complicated given all the required projections of individual isomers onto the CSEs, it is worth noting that many, if not all, of these steps generally take place anyway – simply in a different order – particularly for many commonly encountered non-equilibrium systems.

For example, the present study would imply that, at conditions where *t*-HCOH and *c*-HCOH are not distinct chemical species, any HCOH formed from other chemical reactions (e.g. CH_3 + OH) would have to be projected onto the CSE to determine the fraction of prompt isomerization to CH_2O and onto the IERE

space to determine the fractions of prompt dissociation and prompt reaction with O_2. As per Fig. 8, the primary fate of HCOH would be prompt reaction at combustion temperatures or in any environment where O_2 is appreciably present. Therefore, any reaction like CH_3 + OH forming HCOH could likely just be assumed to produce H + HCO and H_2 + CO or consume O_2 to produce HCOH + O_2 products (which our limited electronic structure calculations imply to be predominantly HCO + HO_2) – with branching fractions that depend on the temperature, pressure, and O_2 mole fraction.

Conclusions

One hundred years ago, Lindemann presented his seminal explanation of the pressure dependence of unimolecular reactions. Namely, reactant molecules with sufficiently short lifetimes (relative to collision times) dissociate more quickly than it takes for collisions to reestablish the Boltzmann distribution of the internal energies of the molecule – yielding pressure-dependent rate constants for unimolecular reactions due to the non-equilibrium reactant energy distributions they induce at low pressures. In the last century, incredible progress has been made in achieving a far greater understanding of and quantitative predictions for unimolecular and (their reverse) association reactions and, in the present day, pressure-dependent phenomenological rate constants are now nearly universally used to describe the rates of unimolecular and associative reactions in phenomenological kinetic modeling that describes the evolution of chemical species.

However, the implications of the Lindemann mechanism for unimolecular reactions may yet be broader – the dissociation-induced non-equilibrium distributions can also impact bimolecular reactions, including non-associative bimolecular reactions, which are generally not considered to have pressure-dependent rate constants. The results from our master equation calculations for the CH_2O/*t*-HCOH/*c*-HCOH + M/O_2 system suggest that even the rate constants for non-associative bimolecular reactions depend on pressure. Specifically, the rate constants for bimolecular reactions can be pressure dependent whenever at least one of its reactants is simultaneously undergoing unimolecular dissociation with pressure-dependent rate constants.

In the present case study, we find that the phenomenological rate constants for bimolecular reactions at 1 atm are significantly lower than the thermal rate constants – even in situations where the bimolecular reaction with O_2 is the dominant consumption pathway and where the traditional rate constant description would not generally be suspected to have significant issues. For example, the phenomenological rate constant for $CH_2O + O_2 = P_{CH2O+O2}$ (R4) at 1 atm is 40% lower than the thermal rate constant at 3000 K, where the CH_2O prompt reaction fraction is less than 1% and the chemically significant eigenvalue is over 100 times lower than the relaxational eigenvalues. The rate constant for $CH_2O + O_2 = P_{CH2O+O2}$ (R4) at 1 atm is nearly 3 times lower than the thermal rate constant at ~4500 K, where the CH_2O prompt reaction fraction is large but the chemically significant eigenvalue is still 10 times lower than the relaxational ones (such that the traditional rate constant description would still not generally be considered problematic[15]).

The reactions $CH_2O + O_2 = P_{t\text{-}HCOH+O2}$ (R5) and $CH_2O + O_2 = P_{c\text{-}HCOH+O2}$ (R6) (involving bimolecular reactions of *t*-HCOH and *c*-HCOH, which are not distinct chemical species under most conditions) are even more strongly influenced by the dissociation-induced non-equilibrium. Correspondingly, the phenomenological rate constants for R5 and R6 at 1 atm are two orders of magnitude lower than those that would be

calculated according to many current treatments of the bimolecular reactivity of molecular entities that are not distinct chemical species.

Altogether, while we present results for a specific reaction system and briefly discuss some of the potential implications, the generality and full implications of this notion are as of yet unclear, and it appears to be a worthwhile subject for future work.

Conflicts of Interest

There are no conflicts to declare.

Acknowledgements

The authors gratefully acknowledge support from the Department of Energy Gas Phase Chemical Physics program (DE-SC0019487) and thank Stephen Klippenstein for sharing the theoretical data for the CH_2O/*t*-HCOH/*c*-HCOH (+M) system.[41]

References and notes

1. F. A. Lindemann, et al. Discussion on 'the radiation theory of chemical action'. *Trans. Faraday Soc.* 17, 598–606 (1922).
2. C. N. Hinshelwood. On the theory of unimolecular reactions. *Proc. R. Soc. Lond. A* 1926, 113, 230–233.
3. B. Widom. Molecular transitions and chemical reaction rates. Science 1965, 148, 1555–1560.
4. D.C. Tardy, B.S. Rabinovitch. Collisional Energy Transfer. Thermal Unimolecular Systems in the Low-Pressure Region. *J. Chem. Phys.* 1966, 45, 3720−3730.
5. B.J. Widom. *Chem. Phys.* 1971, 55, 44-52.
6. B.J. Widom. *Chem. Phys.* 1974, 61, 672-680.
7. J.T. Bartis, B.J. Widom. *Chem. Phys.* 1974, 60, 3474-3482.
8. R.K. Boyd, *J. Chem. Phys.* 1974, 60, 1214-1222.
9. J. Troe. Fall-Off Curves of Unimolecular Reactions. Ber. Bunsenges. Phys. Chem. 1974, 78, 478−488
10. J. Troe. Theory of Thermal Unimolecular Reactions at Low Pressures. I. Solutions of the Master Equation. *J. Chem. Phys.* 1977, 66, 4745−4757.
11. S.J. Klippenstein, J.A. Miller. From the time-dependent, multiple-well master equation to phenomenological rate coefficients. *J. Phys. Chem. A* 2002, 106, 9267–9277.
12. M.J. Pilling, S.H. Robertson. Master equation models for chemical reactions of importance in combustion. *Ann. Rev. Phys. Chem.* 2003, 54, 245–275.
13. J.R. Barker, D.M. Golden. Master Equation Analysis of Pressure-Dependent Atmospheric Reactions. *Chem. Rev.* 2003, 103, 4577−4592.
14. J.A. Miller, S.J. Klippenstein. Master equation methods in gas phase chemical kinetics. *J. Phys. Chem. A* 2006, 110, 10528–10544.
15. J.A. Miller, S.J. Klippenstein. Some Observations Concerning Detailed Balance in Association/Dissociation Reactions. *J. Phys. Chem. A* 2004, 108, 8296-8306.
16. Y. Georgievskii, J.A. Miller, M.P. Burke, S.J. Klippenstein. Reformulation and solution of the master equation for multiple-well chemical reactions. *J. Phys. Chem. A* 117, 12146–12154 (2013).

17. A.W. Jasper, K.M. Pelzer, J.A. Miller, E. Kamarchik, L.B. Harding, S.J. Klippenstein. Predictive a priori pressure-dependent kinetics. *Science* 2014, 346, 1212–1215.
18. Burke, M. P.; Song, R. Evaluating Mixture Rules for Multi-Component Pressure Dependence: H + O_2 (+M) = HO_2 (+M). *Proc. Combust. Inst.* 2017, 36, 245−253
19. Lei, L.; Burke, M. P. Bath Gas Mixture Effects on Multichannel Reactions: Insights and Representations for Systems beyond Single-Channel Reactions. *J. Phys. Chem. A* 2019, 123, 631−649
20. C.F. Goldsmith, M.P. Burke, Y. Georgievskii, S.J. Klippenstein. Effect of Non-Thermal Product Energy Distributions on Ketohydroperoxide Decomposition Kinetics. *Proc. Combust. Inst.* 2015, 35, 283−290.
21. N.J. Labbe, R. Sivaramakrishnan, C.F. Goldsmith, Y. Georgievskii, J.A. Miller, S.J. Klippenstein. Weakly bound free radicals in combustion: "Prompt" dissociation of formyl radicals and its effect on laminar flame speeds. *J. Phys. Chem. Lett.* 2016, 7, 85–89.
22. R.J. Shannon, S.H. Robertson, M.A. Blitz, P.W. Seakins. Bimolecular Reactions of Activated Species: An Analysis of Problematic HC(O)C(O) chemistry. *Chem. Phys. Lett.* 2016, 661, 58−64.
23. A.D. Danilack, S.J. Klippenstein, Y. Georgievskii, C.F. Goldsmith. Low-Temperature Oxidation of Diethyl Ether: Reactions of Hot Radicals across Coupled Potential Energy Surfaces. *Proc. Combust. Inst.* 2021, 38, 671-679.
24. J.A. Miller, R. Sivaramakrishnan, C.F. Goldsmith, M.P. Burke, A.W. Jasper, J. Zádor, N. Hansen, N.J. Labbe, P. Glarborg. Combustion Chemistry in the Twenty-First Century: Developing Theory-Informed Chemical Kinetics Models. *Prog. Energy Combust. Sci.* 2021, 83, 100886.
25. V.D. Knyazev, W. Tsang. Incorporation of Non-Steady-State Unimolecular and Chemically Activated Kinetics into Complex Kinetic Schemes. 1. Isothermal Kinetics at Constant Pressure. J. Phys. Chem. A 1999, 103, 3944-3954.
26. A. Maranzana, J.R. Barker, G. Tonachini. Master Equation Simulations of Competing Unimolecular and Bimolecular Reactions: Application to OH Production in the Reaction of Acetyl Radical with O_2. *Phys. Chem. Chem. Phys.* 2007, 9, 4129−4141.
27. R. Asatryan, G. da Silva, J.W. Bozzelli. Quantum Chemical Study of the Acrolein (CH_2CHCHO) + OH + O2 Reactions. *J. Phys. Chem. A* 2010, 114, 8302−8311
28. D.R. Glowacki, J. Lockhart, M.A. Blitz, S.J. Klippenstein, M.J. Pilling, S.H. Robertson, P.W. Seakins. Interception of Excited Vibrational Quantum States by O_2 in Atmospheric Association Reactions. *Science* 2012, 337, 1066−1069.
29. M. Pfeifle, M. Olzmann. Consecutive Chemical Activation Steps in the OH-Initiated Atmospheric Degradation of Isoprene: An Analysis with Coupled Master Equations. *Int. J. Chem. Kinet.* 2014, 46, 231−244.
30. M.P. Burke, C.F. Goldsmith, Y. Georgievskii, S.J. Klippenstein. Towards a Quantitative Understanding of the Role of Non-Boltzmann Reactant Distributions in Low Temperature Oxidation. *Proc. Combust. Inst.* 2015, 35, 205−213.
31. M.P. Burke, S.J. Klippenstein, S. J. Ephemeral Collision Complexes Mediate Chemically Termolecular Transformations that Affect System Chemistry. *Nat. Chem.* 2017, 9, 1078−1082.
32. M.C. Barbet, K. McCullough, M.P. Burke. A Framework for Automatic Discovery of Chemically Termolecular Reactions. *Proc. Combust. Inst.* 2019, 37, 347−354.
33. A.W. Jasper, R. Sivaramakrishnan, S.J. Klippenstein. Nonthermal Rate Constants for CH_4* + X → CH_3 + HX, X = H, O, OH, and O_2. *J. Chem. Phys.* 2019, 150, 114112.

34. L. Lei, M.P. Burke. Understanding and representing the distinct kinetics induced by reactive collisions of rovibrationally excited ephemeral complexes across reactive collider mole fractions and pressures. *J. Phys. Chem. A* 2020, 120, 10937–10953.
35. R.E. Cornell, M.C. Barbet, M.P. Burke. Automated Discovery of Influential Chemically Termolecular Reactions in Energetic Material Combustion: A Case Study for RDX. *Proc. Combust. Inst.* 2021, 38, 787-794.
36. L. Lei, M.P. Burke. An Extended Methodology for Automated Calculations of Non-Boltzmann Kinetic Sequences: H + C_2H_2 + X and Combustion Impact. *Proc. Combust. Inst.* 2021, 38, 661-669.
37. J.A. Miller, S.J. Klippenstein. Determining phenomenological rate coefficients from a time-dependent, multiple-well master equation: "Species reduction" at high temperatures. *Phys. Chem. Chem. Phys.* 2013, 15, 4744–4753.
38. S.J. Klippenstein. From theoretical reaction dynamics to chemical modeling of combustion. *Proc. Combust. Inst.* 2017, 36, 77-111.
39. C.F. Goldsmith, W.H. Green, S.J. Klippenstein. Role of O_2 + QOOH in Low-Temperature Ignition of Propane. 1. Temperature and Pressure Dependent Rate Coefficients. *J. Phys Chem. A* 2012, 116, 3325−3346.
40. L.P. Maffei, M. Pelucchi, C. Cavallotti, A. Bertolino, T. Faravelli. Master equation lumping for multi-well potential energy surfaces: a bridge between ab initio based rate constant calculations and large kinetic mechanisms. *Chem. Eng. J.* 2021, 422, 129954.
41. S.J. Klippenstein, in preparation.
42. V. Vasudevan, D.F. Davidson, R.K. Hanson, C.T. Bowman, D.M. Golden. High-Temperature Measurements of the Rates of the Reactions CH_2O + Ar → Products and CH_2O + O_2 → Products. *Proc. Combust. Inst.* 2007, 31, 175−183.
43. H. Teitelbaum, A. Lifshitz. Non-equilibrium kinetics of bimolecular reactions. Part 7: The puzzle of the H + O_2 reaction. *Phys. Chem. Chem. Phys.,* 2000, 2, 687-692.
44. At any specific conditions where *t*-HCOH and *c*-HCOH are not well-defined chemical species, treating their reactivity in phenomenological kinetic models does not require them to be among the considered species if their reactivity is instead treated via prompt isomerization/dissociation/bimolecular reactions and well-skipping pathways corresponding to chemically termolecular reactions and the bimolecular reaction of the CH_2O, or more specifically the λ_1 eigenmode, with O_2 (e.g. as performed for the results presented in this paper).

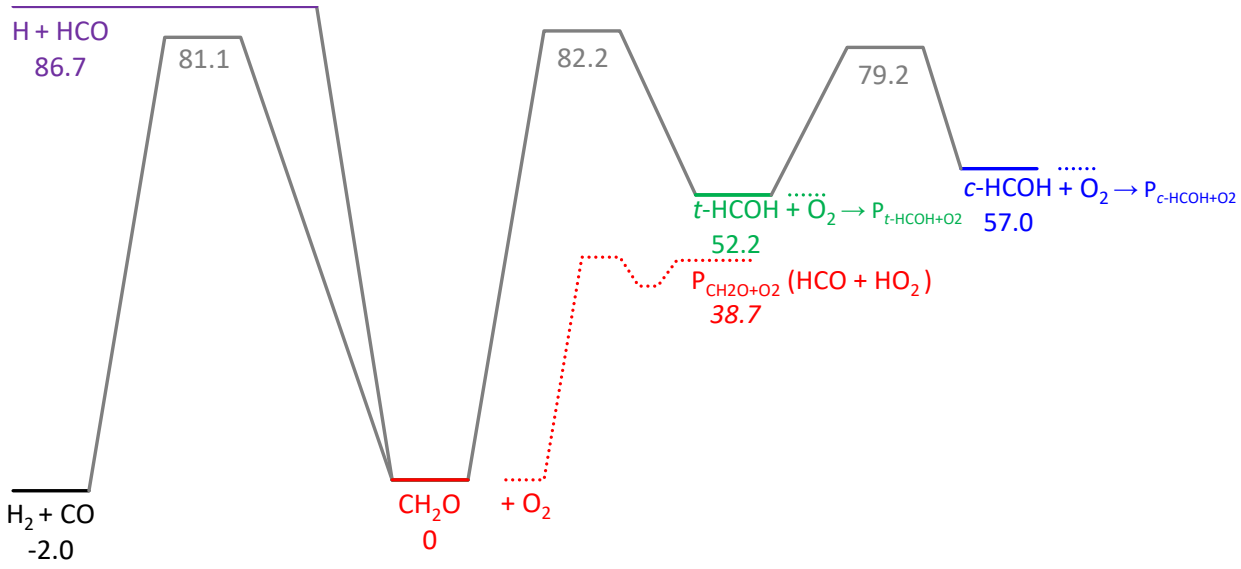

Figure 1. Potential energy surface for the unimolecular kinetics of CH_2O (including its dissociation to bimolecular products and isomerization to *t*-HCOH and *c*-HCOH)[41] and the bimolecular reactions of CH_2O, *t*-HCOH, and *c*-HCOH with O_2. The energies are listed in units of kcal/mol.

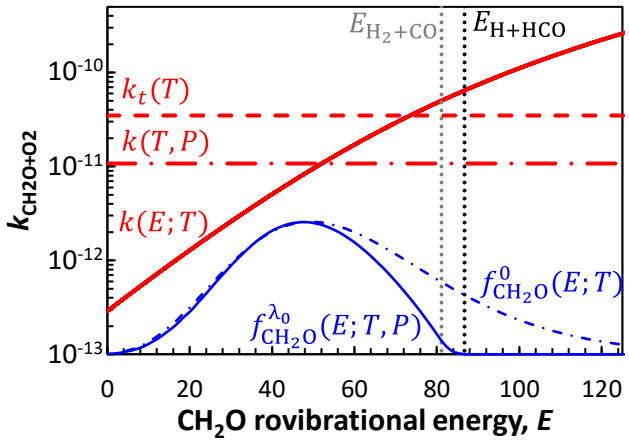

Figure 2. Illustration of the mechanism for pressure dependence in bimolecular reaction rate constants due to dissociation-induced non-equilibrium reactant energy distributions. The red lines compare the semi-microcanonical rate constant for CH_2O with rovibrational energy *E* reacting with O_2 at 5000 K to yield product $P_{CH2O+O2}$, labeled $k(E;T)$; the phenomenological rate constant for CH_2O + O_2 to yield product $P_{CH2O+O2}$ at 5000 K and 1 atm, $k(T,P)$; the thermal (high-pressure-limit) rate constant for CH_2O + O_2 to yield product $P_{CH2O+O2}$ at 5000 K, labeled $k_\infty(T)$. The blue lines compare the energy distribution of CH_2O in the slowest chemically significant eigenvector at 1 atm and 5000 K, labeled $f^{\lambda_0}_{CH_2O}(E;T,P)$; and the Boltzmann distribution for CH_2O at 5000 K, $f^{(0)}_{CH_2O}(E;T)$. For reference, the energy thresholds for CH_2O → H_2 + CO and CH_2O → H + HCO are indicated by the dotted lines, labeled E_{H_2+CO} and E_{H+HCO}.

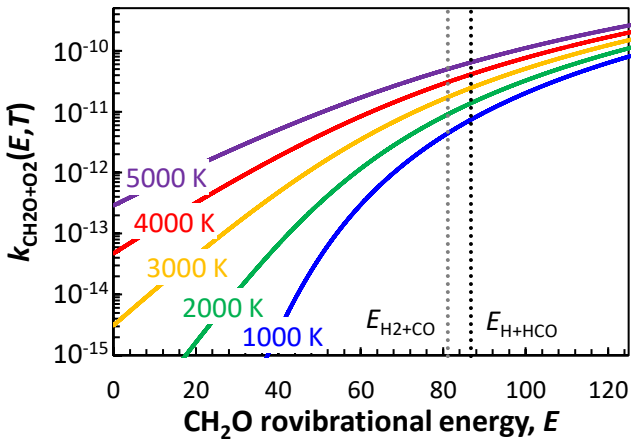

Figure 3. Rate constant for CH_2O with rovibrational energy E reacting with O_2 at various temperatures (as indicated) as a function of E. For reference, the energy thresholds for $CH_2O \rightarrow H_2 + CO$ and $CH_2O \rightarrow H + HCO$ are indicated by the dotted lines.

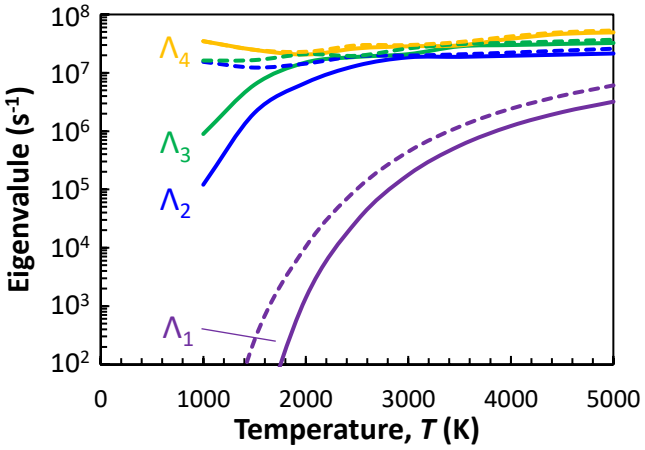

Figure 4. The four smallest eigenvalues for the CH_2O/*t*-HCOH/*c*-HCOH + M/O_2 reaction system vs. temperature for a pressure of 1 atm and O_2 mole fractions of 10^{-7} (solid lines, representative of the low O_2 limit) and 0.209 (dashed lines, representative of air).

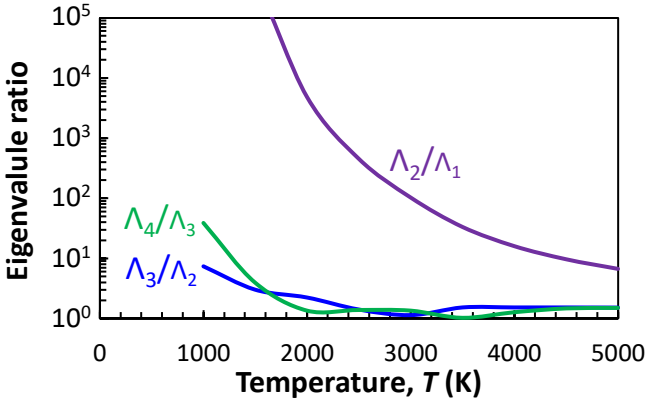

Figure 5. Ratios among the four smallest eigenvalues for the CH_2O/*t*-HCOH/*c*-HCOH + M/O_2 reaction vs. temperature for a pressure of 1 atm and O_2 mole fraction of 10^{-7} (representative of the low O_2 limit).

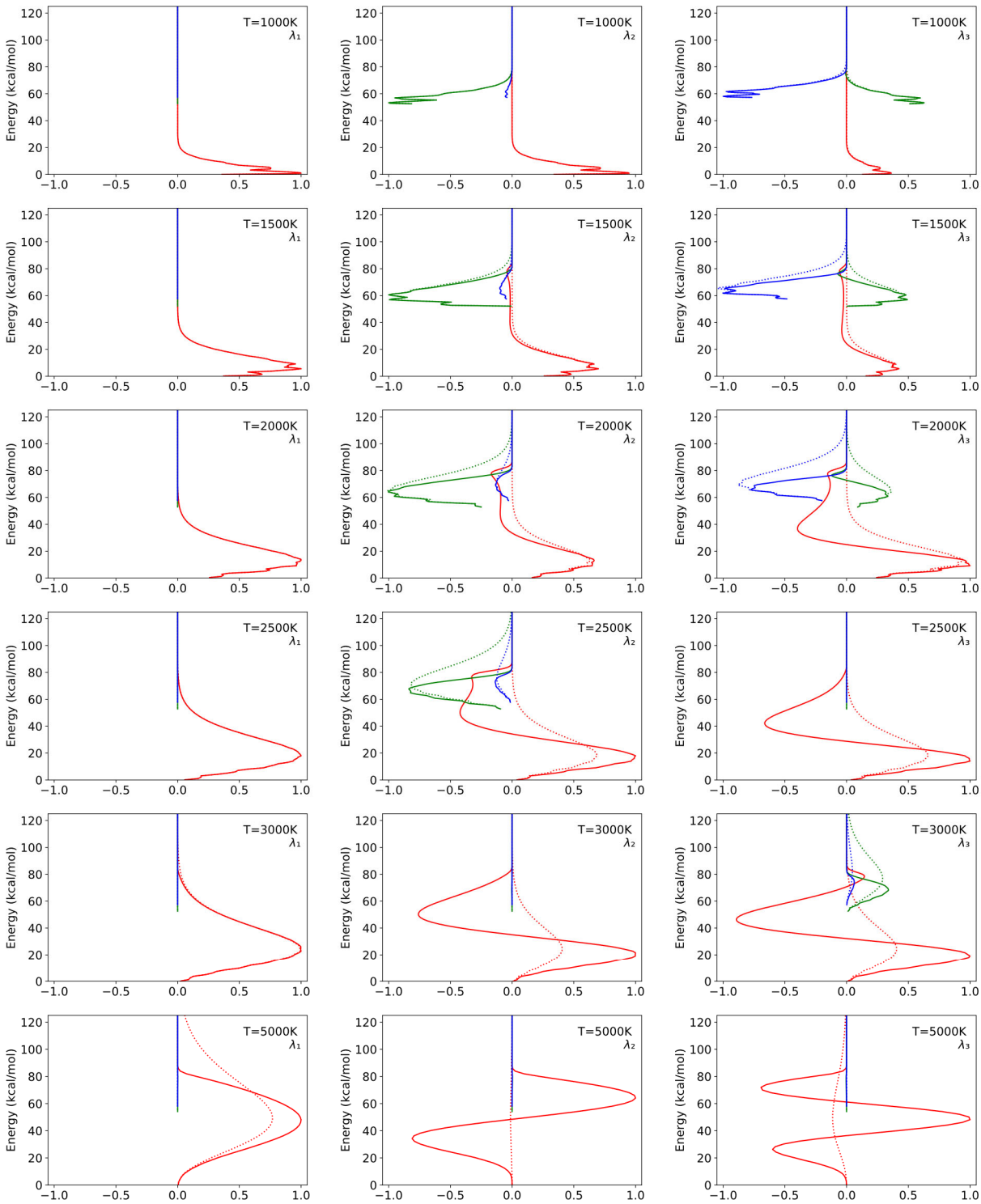

Figure 6. The energy-resolved amplitudes (x-axis) of each isomer for the three eigenvectors with the smallest eigenvalues across varied temperatures, a pressure of 1 atm, and O_2 mole fraction of 10^{-7} (representative of the low O_2 limit) as a function of rovibrational energy (y-axis). Solid lines indicate amplitudes of CH_2O (red), *t*-HCOH (green), and *c*-HCOH (blue) in each eigenvector. Dotted lines indicate the corresponding Boltzmann distributions for each isomer scaled to match the amplitude of each isomer in the eigenvector at the lowest energy of each isomer, E_{0i}, such that $\left(f_i^{(\lambda)}(E_{0i})/f_i^{(0)}(E_{0i})\right) f_i^{(0)}(E)$ is plotted.

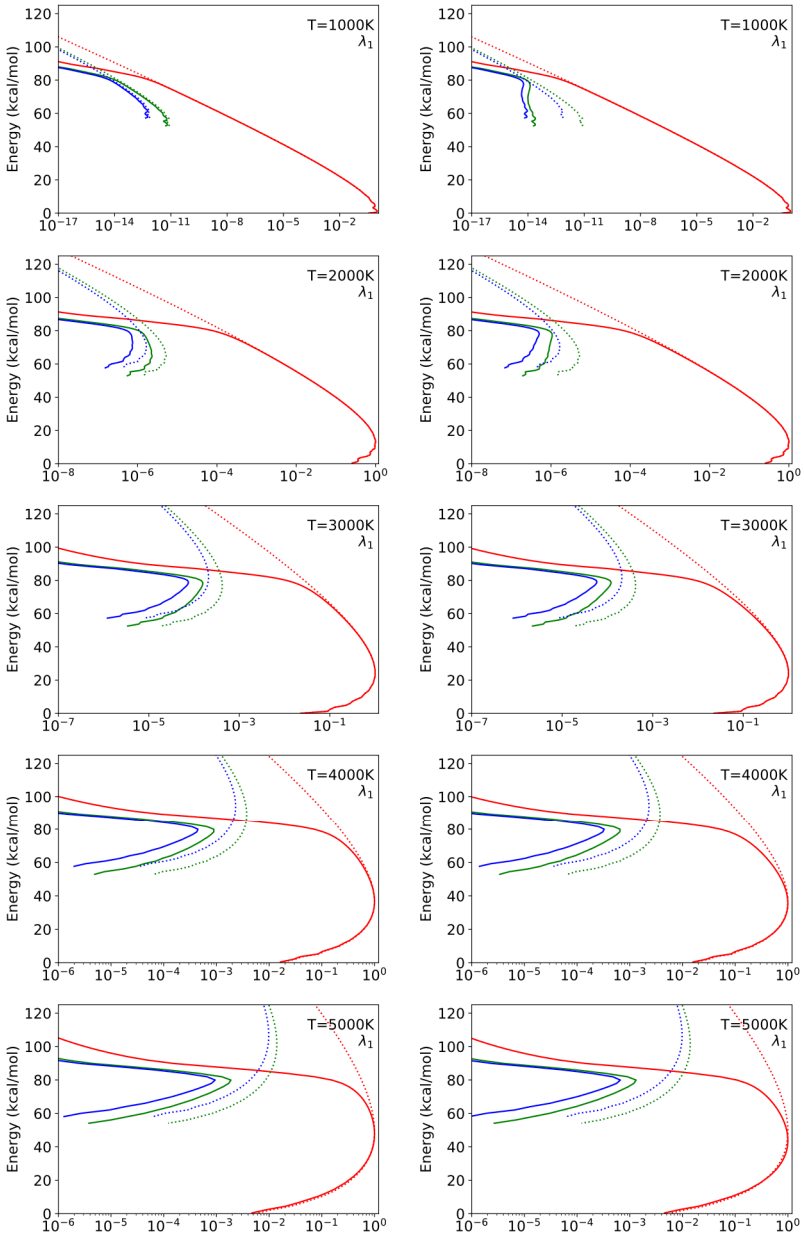

Figure 7. The energy-resolved amplitudes (x-axis) of each isomer for the eigenvector with the smallest eigenvalue across varied temperatures for a pressure of 1 atm and (left) O_2 mole fraction of 10^{-7} (representative of the low O_2 limit) and (right) O_2 mole fraction of 0.209 (representative of air) as a function of rovibrational energy (y-axis). Solid lines indicate amplitudes of CH_2O (red), *t*-HCOH (green), and *c*-HCOH (blue) in each eigenvector. Dotted lines indicate the corresponding Boltzmann distributions for each isomer with different scalings than Fig. 6. For CH_2O, the Boltzmann populations are scaled to match the maximum amplitude of CH_2O in the eigenvector, i.e. $\left(\max\left[f^{(\lambda)}_{\mathrm{CH_2O}}(E)\right] / \max\left[f^{(0)}_{\mathrm{CH_2O}}(E)\right]\right) f^{(0)}_{\mathrm{CH_2O}}(E)$. For *i* = *t*-HCOH and *c*-HCOH, the Boltzmann populations are scaled to represent their values if they were in chemical equilibrium with CH_2O, i.e. $\left(\max\left[f^{(\lambda)}_{\mathrm{CH_2O}}(E)\right] / \max\left[f^{(0)}_{\mathrm{CH_2O}}(E)\right]\right)\left\{\left(\mathrm{sum}\left[f^{(0)}_{\mathrm{CH_2O}}(E)\right] / \mathrm{sum}\left[f^{(0)}_{t-\mathrm{HCOH}}(E)\right]\right)K_{eq,13}\right\} f^{(0)}_{t-\mathrm{HCOH}}(E)$ and $\left(\max\left[f^{(\lambda)}_{\mathrm{CH_2O}}(E)\right] / \max\left[f^{(0)}_{\mathrm{CH_2O}}(E)\right]\right)\left\{\left(\mathrm{sum}\left[f^{(0)}_{\mathrm{CH_2O}}(E)\right] / \mathrm{sum}\left[f^{(0)}_{c-\mathrm{HCOH}}(E)\right]\right)K_{eq,14}\right\} f^{(0)}_{c-\mathrm{HCOH}}(E)$, respectively.

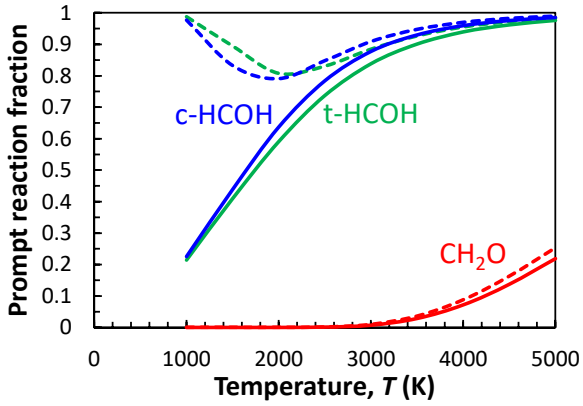

Figure 8. Fraction of CH_2O, *t*-HCOH, and *c*-HCOH that would promptly dissociate or react with O_2 if formed with rovibrational energies following the Boltzmann distribution as a function of temperature for a pressure of 1 atm and O_2 mole fractions of 10^{-7} (solid lines) and 0.209 (dashed lines).

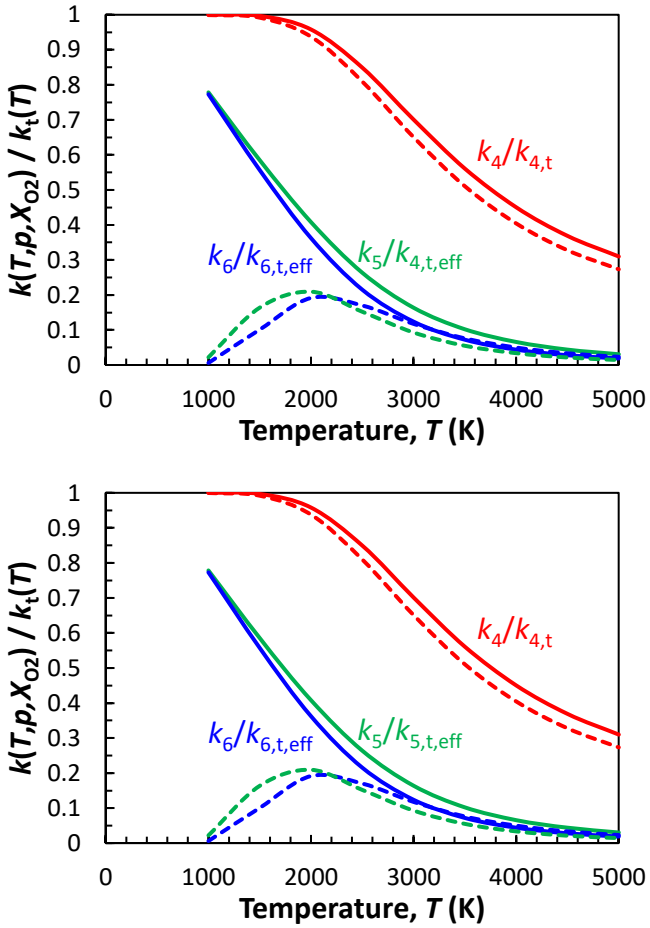

Figure 9. Phenomenological rate constants, $k(T,P,X_{O2})$, for $CH_2O + O_2 \leftrightarrow P_{CH2O+O2}$ (R4), $CH_2O + O_2 \leftrightarrow P_{t\text{-}HCOH+O2}$ (R5), and $CH_2O + O_2 \leftrightarrow P_{c\text{-}HCOH+O2}$ (R6) for a pressure of 1 atm and O_2 mole fractions of 10^{-7} (solid lines) and 0.209 (dashed lines) relative to their (effective) thermal rate constants, $k_t(T)$.

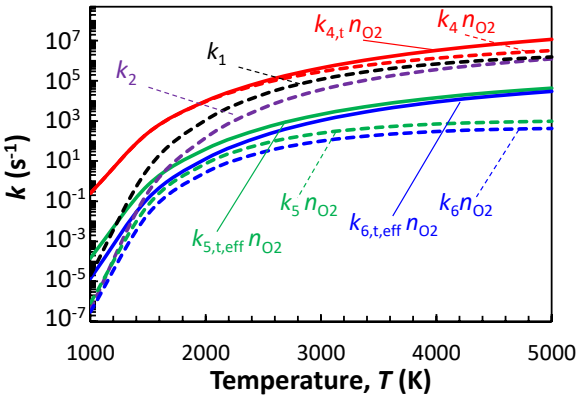

Figure 10. Comparison of rate constants across various temperatures for a pressure of 1 atm and O_2 mole fraction of 0.209 (representative of air): phenomenological rate constants, $k(T,P,X_{O2})$ for CH_2O to form H_2 + CO (R1) and H + HCO (R2); pseudo-first-order phenomenological rate constants, $k(T,P,X_{O2})n_{O2}$, for CH_2O ($+O_2$) to form $P_{CH2O\ +O2}$ (R4), $P_{t\text{-}HCOH+O2}$ (R5), and $P_{c\text{-}HCOH+O2}$ (R6); and pseudo-first-order (effective) thermal rate constants, $k_t(T)n_{O2}$, for R4, R5, and R6.

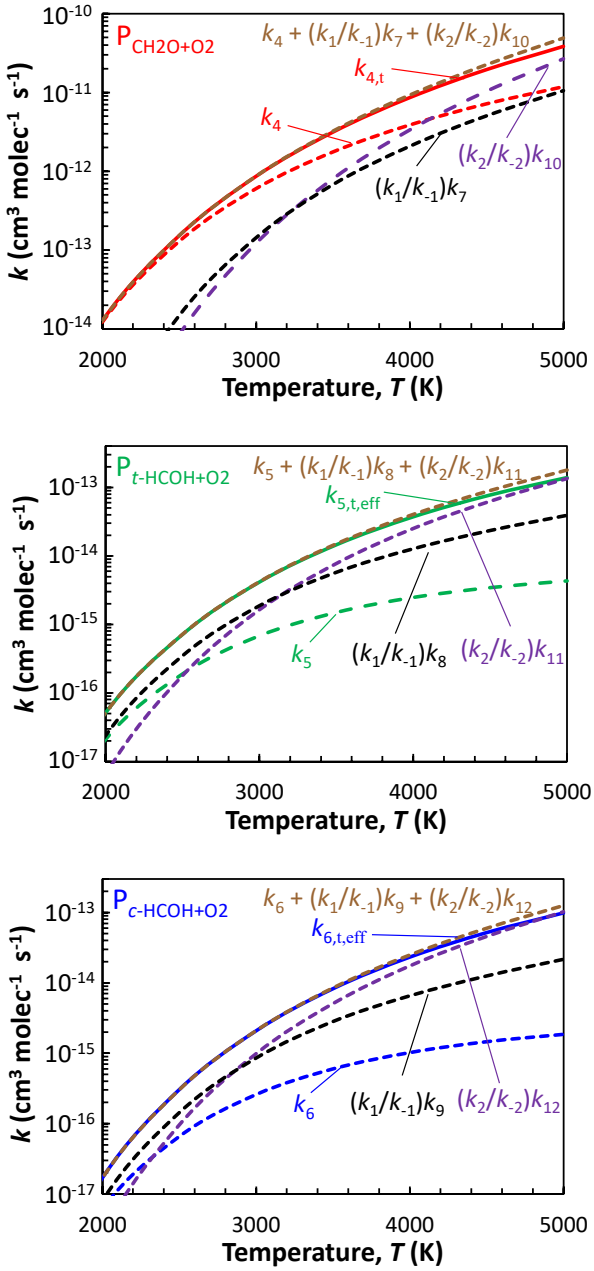

Figure 11. Comparison of rate constants across various temperatures for a pressure of 1 atm and O_2 mole fraction of 10^{-7} (representative of the low O_2 limit): (effective) thermal rate constants for $CH_2O + O_2$; phenomenological rate constants for $CH_2O + O_2$; and phenomenological rate constants for $H_2 + CO + O_2$ and $H + HCO + O_2$ times the ratio of the rate constants for R1 and R-1 and R2 and R-2, respectively (representing the contribution from chemically termolecular reactions when CH_2O is equilibrated with its bimolecular fragments via R1 and R2); and the sum of bimolecular and chemically termolecular reaction contributions to $CH_2O + O_2$ at equilibrium.